# Synthesis, Characterization, and Lithium Battery Applications of Molybdenum Oxysulfides

K. M. Abraham* and D. M. Pasquariello

*EIC Laboratories, Inc., Norwood, Massachusetts 02062*

*Received February 26, 1993. Revised Manuscript Received July 6, 1993®*

Molybdenum oxysulfides, $MoO_xS_y$, obtained by thermal decomposition of $(NH_4)_2MoO_2S_2$, have been identified as Li insertion positive electrodes for rechargeable Li batteries. The compositions of the oxysulfides and their discharge capacity and rechargeability in Li cells were influenced by the temperature at which they were formed from $(NH_4)_2MoO_2S_2$. Thermolysis of the latter in the 200–380 °C range appeared to occur by a solid-state polymerization reaction, wherein the $MoO_xS_y$ formed at different temperatures can be viewed as polymers with different chain lengths. $MoO_xS_y$ prepared at 200, 300, and 380 °C and in a two-step 200/380 °C thermolysis, respectively, exhibited first discharge capacity, in Li cells, equivalent to the incorporation of 2.70, 2.80, 1.90, and 1.30 Li per molybdenum. These capacities translated into quasi-theoretical specific energies from 290 to 685 W h/kg for the Li cells. A fraction of the capacity in the first discharge of $Li/MoO_xS_y$ cells was irreversible, and it is largely attributed to a phase change accompanying Li insertion into the material. $MoO_xS_y$ obtained by the decomposition of an intimate 1:1 mixture of $(NH_4)_2MoO_4$ and $(NH_4)_2MoS_4$ at 380 °C exhibited electrochemical behavior reminiscent of the Mo–oxysulfide obtained by decomposition of $(NH_4)_2MoO_2S_2$ at the same temperature.

## Introduction

Transition-metal chalcogenides have been widely investigated as cathodes for ambient temperature rechargeable Li batteries.[1,2] Prominent examples include $TiS_2$, $NbSe_3$, and $MoS_2$ which undergo solid-state topochemical (insertion) reactions with Li. The cathode discharge reaction of these Li batteries involves a double injection of $Li^+$ and electrons into the vacant crystallographic lattice sites and the conduction bands, respectively, of the chalcogenide hosts. The reverse processes take place during recharge of the battery. AA-size Li cells based on these three chalcogenide cathodes represent early attempts to commercialize secondary Li batteries.[3] These potential energy sources for a variety of consumer equipment are characterized by specific energies of 60 to 130 W h/kg and energy densities of 150–300 W h/L. The constantly evolving transportation, portable communication, and computer technologies, however, are demanding more and more energy dense batteries, and as a result, the search for new and imporved positive electrode (cathode) materials continues. In this regard, molybdenum chalcogenides have received a great deal of attention. They include the Chevrel phases of general formula $M_yMo_6X_8$ (M = metallic element, X = chalcogen),[4] amorphous $MoS_3$,[1,5,6] $Mo_2S_5$,[6] and $MoSe_3S$.[7,8] This paper reports the results of an extension of this search for improved cathode materials to a previously unexplored class of molybdenum compounds, namely molybdenum oxysulfides. A preliminary communication on the electrochemistry of these materials has appeared.[9] In this paper we present a more detailed account of the mechanism of formation of Mo oxysulfides from ammonium dithiomolybdate ($(NH_4)_2MoO_2S_2$) along with their electrochemistry in Li cells. We have also found that a molybdenum oxysulfide obtained from the thermal decomposition of an intimate, equimolar, mixture of $(NH_4)_2MoO_4$ and $(NH_4)_2MoS_4$, in the solid-state, showed electrochemical behavior similar to that obtained from $(NH_4)_2MoO_2S_2$ at the same temperature. It is also important to note that the chemistry and electrochemistry of molybdenum sulfides and oxysulfides are important in chemical catalysis,[10] particularly the dehydrosulfurization process.

## Experimental Procedures

All experiments were carried out in the absence of air and moisture either in a Vacuum Atmospheres Corporation argon-filled drybox or using standard techniques employed in the manipulation of air-sensitive compounds.[11]

Ammonium paramolybdate ($(NH_4)_6Mo_7O_{24}\cdot 4H_2O$, Fisher), concentrated ammonium hydroxide ($NH_3$(aq), Fisher), and hydrogen sulfide ($H_2S$, Matheson) were reagent grade, and used as-received. Propylene carbonate (PC) obtained from Burdick & Jackson was dried over 4-Å molecular sieves and distilled under a reduced pressure of 1 mmHg. Lithium perchlorate ($LiClO_4$, Alfa) was dried under vacuum at 110 °C. Tetrahydrofuran (THF), 2-methyltetrahydrofuran (2-MeTHF), and 2-methylfuran (2-MeF), all obtained from Aldrich, were distilled from calcium hydride under argon. Lithium hexafluoroarsenate ($LiAsF_6$, Lithco) was used as-received.

® Abstract published in *Advance ACS Abstracts*, September 1, 1993.

(1) Whittingham, M. S. *Prog. Solid-State Chem.* **1978**, *12*, 41.
(2) Abraham, K. M. *J. Power Sources* **1981**, *7*, 1.
(3) Abraham, K. M. In *Proceedings of the Electrochemical Society Softbound Proceedings Volume*; Subbarao, S., et al., Eds.; The Electrochemical Society; Pennington, NJ; 1990; PV90-5, 1.
(4) Cava, R. J.; Santoro, A.; Tarascon, J. M. *J. Solid State Chemistry* **1984**, *54*, 193.
(5) Harris, P. B.; Holleck, G. L.; Buzby, J.; Avery, J.; Pitts, L.; Abraham, K. M. Technical Report No. 9 on ONR Contract N00014-77-C-0155, 1982.
(6) Jacobson, A. J.; Chianelli, R. R.; Rich, S. M.; Whittingham, M. S. *Mater. Res. Bull.* **1979**, *14*, 1437.
(7) Pasquariello, D. M.; Abraham, K. M. *Mater. Res. Bull.* **1987**, *22*, 37.
(8) Abraham, K. M.; Pasquariello, D. M.; McAndrews, G. F. *J. Electrochem. Soc.* **1987**, *134*, 2661.
(9) Abraham, K. M.; Pasquariello, D. M.; Willstaedt, E. B. *J. Electrochem. Soc.* **1992**, *136*, 576.
(10) Chianelli, R. R. *Int. Rev. Phys. Chem.* **1982**, *2*, 127.
(11) Shriver, D. F. *The Manipulation of Air-Sensitive Compounds*; McGraw-Hill: New York, 1969.

0897-4756/93/2805-1233$04.00/0 

**Characterization of Materials.** Physical characterization of the precursors and decomposition products involved X-ray diffraction analysis with a Rigaku diffractometer, thermogravimetric analysis (TGA) with a Perkin-Elmer DSC/TGA 7 analyzer, Fourier transform infrared spectroscopic analysis (FTIR) with an IBM System 9000 FTIR spectrometry, UV–visible spectroscopy with a Cary 14 spectrophotometer, elemental analysis (Galbraith Laboratories, Knoxville, TN), and electron spectroscopy for chemical analysis (ESCA) by Perkin-Elmer Physical Electronics Laboratory, Eden Prairie, MN.

**Preparation of $(NH_4)_2MoS_4$.** Ammonium tetrathiomolybdate was prepared as described before[12] by bubbling $H_2S$ through 60 g of ammonium paramolybdate [$(NH_4)_6Mo_7O_{24}\cdot 4H_2O$] dissolved in 300 mL of concentrated $NH_3$(aq), at room temperature. A yellow solid (ammonium dithiomolybdate) formed in the reaction vessel redissolved with continued passing of $H_2S$ and, subsequently, an orange solid precipitated out. This precipitate was filtered, washed with cold $NH_3$(aq) and dried in vacuum.

**Preparation of $(NH_4)_2MoO_2S_2$.** Ammonium dithiomolybdate was prepared using the same procedure as described above except that the yellow precipitate which was first formed upon bubbling $H_2S$ was collected. It was washed with $NH_3$(aq) that had been cooled to 0 °C and dried in vacuum. It exhibited an X-ray powder diffraction pattern identical that reported in the literature.[13] Elemental analysis: calcd N 12.3%, H 3.5%, Mo 42.9%, O 14.0%, S 28.1%; found N 11.4%, H 3.3%, Mo 42.3%, O 17.2%, S 25.6%.

The filtrate after the removal of $(NH_4)_2MoO_2S_2$ was cooled to 0 °C to obtain a second batch of the thiomolybdate. When the remaining filtrate was dried under vacuum, another batch of orange-yellow crystals was obtained which was identified to be mostly $(NH_4)_2MoO_3S$ with small amounts of $(NH_4)_2MoS_4$ and $(NH_4)_2MoO_2S_2$. Elemental analysis for $(NH_4)_2MoO_3S$: calcd N 13.2%, H 3.8%, Mo 45.3%, O 22.6%, S 15.1%; found N 8.7%, H 2.7%, Mo 47.9%, O 22.1%, S 15.0%. These three materials can be distinguished in a mixture from their characteristic absorptions in the UV–visible range.[14]

**Preparation of Molybdenum Oxysulfides.** A weighed amount of $(NH_4)_2MoO_2S_2$, contained in a quartz boat, was heated in an atmosphere of flowing argon at a temperature selected from the range 200–380 °C. The mixture was heated for 3 h at the selected temperature during which time a constant weight was achieved. The compositions of the materials prepared from the different heat treatments are discussed in the Results and Discussion.

A molybdenum oxysulfide was also prepared from a mixture of $(NH_4)_2MoS_4$ and $(NH_4)_6Mo_7O_{24}\cdot 4H_2O$ taken in 1:1 mole ratio by the metal. The mixture was first prepared by mixing solutions of $(NH_4)_2MoS_4$ and $(NH_4)_6Mo_7O_{24}$ in $NH_3$(aq), evaporating to dryness, then decomposing the solid residue at 300 °C.

**Electrochemical Evaluation of Oxysulfides.** Electrochemistry of the oxysulfides as it relates to their use as cathodes in secondary Li cells was performed using procedures developed in this laboratory and described elsewhere.[7,8]

A laboratory Li test cell consisted of a cathode of the oxysulfide flanked on either side by a Li foil anode, the two electrodes being separated by a porous Celgard polypropylene separator. The cathode, measuring 2.5 cm × 4 cm × 0.06 cm was prepared from a mixture of 60 wt % of the oxysulfide, 30 wt % Shawinigan acetylene black carbon, and 10 wt % Teflon. This mixture was suspended in cyclohexane and then pasted on an expanded metal screen which served as the current collector. The carbon was used in the cathode for providing electronic conductivity to the electrode, and Teflon served as the binder. The electrode package was housed in a stainless steel D-cell can and the cell was filled with electrolyte and hermetically sealed by Tig welding. Two electrolyte solutions were used: (i) $LiAsF_6$ (1.5 M) dissolved in a mixture of tetrahydrofuran, 2-methyltetrahydrofuran, and 2-methylfuran (48:48:4 percent by volume),[15] (ii) $LiClO_4$ (1 M) dissolved in propylene carbonate (PC). The latter solution was used when it was necessary to discharge the cell to potentials below 1.6V versus $Li^+$, since the first electrolyte undergoes reduction at such low potentials.

**Table I. Weight Loss vs Temperature for Selected Points on the $(NH_4)_2MoO_2S_2$ TGA Curve**

| temp (°C) | % wt loss | temp (°C) | % wt loss |
|---|---|---|---|
| 190 | 16.9 | 439 | 23.5 |
| 320 | 21.3 | 550 | 31.8 |

The cells were discharged and charged using either a stepped-potential cycling technique[8] or galvanostatically. The former allowed precise determination of the Li insertion capacity of the oxysulfide cathode material over a given potential range in which the stepped-potential technique involves a computer controlled potentiostatic sweep of the desired potential range. The potential of the cathode is changed by a selected step value ($dV$), and the resulting current is allowed to decay until it reaches a predetermined cutoff limit. This limit is usually a low current (e.g., 10 μA), in effect allowing a close approximation of the equilibrium potential. At this point the next potential step is made, with the capacity at each potential step (differential capacity, $dQ$) determined by integration of the current–time curve. A graph of the individual step capacities ($dQ/dV$) as a function of the cell potential ($V$) is useful to detect phase transitions in the cathode material. For this, the data from discharge and charge are combined and plotted in a manner similar to a cyclic voltammogram (CV). If the reaction occurs at a single potential step, a sharp peak will be observed in the $dQ/dV$ *vs* $V$ curve, whereas a broad current peak will be obtained if the reaction occurs over a wide potential range. The results are also plotted as potential versus capacity, similar to those obtained from galvanostatic cycling. The galvanostatic technique was used for the long-term discharge/charge cycling of Li cells. The current density usually was 0.5 mA/cm², and the potential limits for each charge and discharge are given in the relevant figures.

**Li Insertion Capacity of Oxysulfides.** Lithium insertion capacity of the oxysulfides was determined via the *n*-butyllithium (*n*-BuLi) technique.[16] Typically 0.5 g of the oxysulfide was stirred with a large excess of *n*-BuLi in hexane. After contact for about 1 week, the solid was filtered. The filtrate was hydrolyzed with $H_2O$ and titrated against a standard solution of HCl to determine the amount of unreacted *n*-BuLi. The difference provided the amount of *n*-BuLi reacted/mol of the oxysulfide.

## Results and Discussion

**Mechanism of Formation and Compositions of Molybdenum Oxysulfides.** It is well established[14] that the thiomolybdates, $(NH_4)_2MoO_3S$, $(NH_4)_2MoO_2S_2$, $(NH_4)MoOS_3$, and $(NH_4)_2MoS_4$ are formed when $H_2S$ is bubbled through an ammoniacal solution of ammonium paramolybdate (which in aqueous solutions can be represented as $(NH_4)_2MoO_4$)). The solutions of the thiomolybdate exhibit characteristic UV–visible absorption peaks: $(NH_4)_2MoO_3S$ at 288 and 392 nm; $(NH_4)MoO_2S_2$ at 288, 319, and 394 nm; $(NH_4)_2MoOS_3$ at 243, 270, 319, 392, and 460 nm and $(NH_4)_2MoS_4$ at 241, 316, and 463 nm. We have found that $(NH_4)_2MoO_3S$, $(NH_4)_2MoO_2S_2$, and $(NH_4)_2MoS_4$ can be isolated as pure materials. The X-ray diffraction pattern of $(NH_4)_2MoO_2S_2$ agreed very well with that reported in the literature,[13] and the absence of lines due to any other materials indicated that impurities, including the other thiomolybdates, were less than 5 wt %. The thermal decomposition of the thiomolybdates is believed to yield

(12) Spengler, B.; Weber, A., *Chem. Ber.* **1989**, *92*, 2163.
(13) ASTM Reference Data File No. 23-786. See also: Von Müller, A.; Diemann, E.; Baran, E. J. *Z. Anorg. Allg. Chem.* **1970**, *375*, 87.
(14) Tsigdinos, G. A. Inorganic Sulfur Compounds of Molybdenum and Tungsten: Their Preparation, Structure and Properties *Top. Curr. Chem.* **1978**, *76*, 65.
(15) Abraham, K. M.; Pasquariello, D. M.; Martin, F. J. *J. Electrochem. Soc.* **1986**, *133*, 643.
(16) Dines, M. B. *Mater. Res. Bull.* **1975**, *10*, 287.

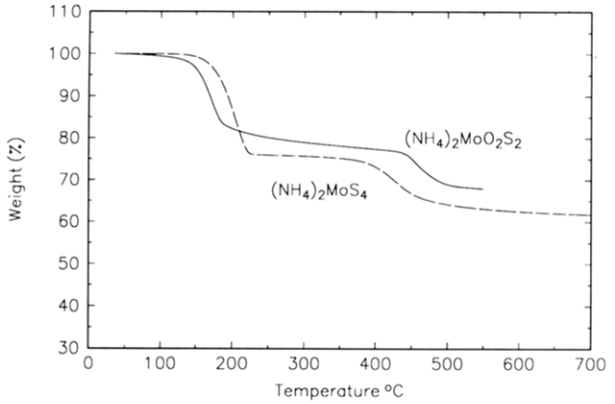


**Figure 1.** TGA curves of $(NH_4)_2MoS_4$ and $(NH_4)_2MoO_2S_2$. The heating rate was 5 °C/min.

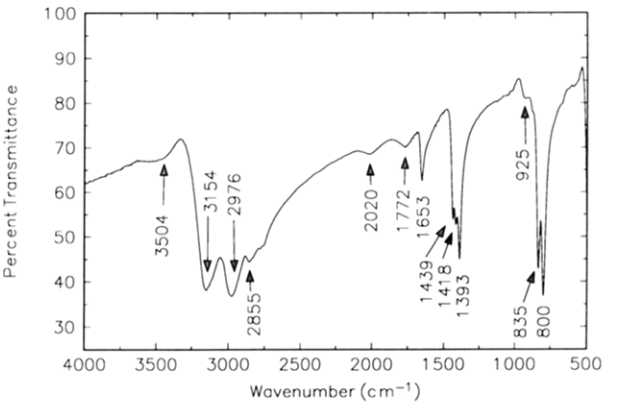


**Figure 2.** FTIR spectrum of $(NH_4)_2MoO_2S_2$.

$MoO_2S$, $MoOS_2$, and $MoS_3$[6,14,17] per eqs 1–3.

$$(NH_4)_2MoO_3S \xrightarrow[\Delta]{} 2NH_3 + H_2O + MoO_2S \quad (1)$$

$$(NH_4)_2MoO_2S_2 \xrightarrow[\Delta]{} 2NH_3 + H_2O + MoOS_2 \quad (2)$$

$$(NH_4)_2MoS_4 \xrightarrow[\Delta]{} 2NH_3 + H_2S + MoS_3 \quad (3)$$

The formation of $MoO_2S$ and $MoOS_2$ in the reactions of eqs 1 and 2, instead of $MoO_3$, and $MoO_2S$, respectively, is sound on thermodynamic grounds since the evolution of $H_2O$ is more exothermic than that of $H_2S$. On the other hand, a careful examination of the structure and properties of the decomposition products of $(NH_4)_2MoO_2S_2$ indicates that the thiomolybdate decomposition is temperature dependent and results in a variety of oxysulfides with nonstoichiometric compositions and unique electrochemical properties. As we show below, at least at higher temperatures (viz. ~380 °C), the decomposition of $(NH_4)_2MoO_2S_2$ appears to lead to the evolution of both $H_2S$ and $H_2O$. We have examined the thermal decomposition of $(NH_4)_2MoO_3S$ also, albeit briefly.[9] The theoretical elemental composition of $(NH_4)_2MoO_3S$ is 13.2% N, 3.8% H, 45.3 Mo, 22.6% O, 15.1% S. The material which we prepared had the composition 8.7% N, 2.7% H, 47.9% Mo, 22.1% O, and 15.0% S; decomposition at 300 °C yielded a product with the elemental composition of 58.5% Mo, 16.7% O, 18.7% S, which corresponds to a nominal stoichiometry of $MoO_2S$.

The thermograms illustrating the decompositions of $(NH_4)_2MoS_4$ and $(NH_4)_2MoO_2S_2$ are presented in Figure 1. The weight losses of 24.4% and 37.5% for $(NH_4)_2MoS_4$ at 300 and 500 °C, respectively, are in good agreement with the reactions represented by eqs 3 and 4. On the other hand, the compositions of the thermolysis products of $(NH_4)_2MoO_2S_2$ are more temperature sensitive. The weight losses at four different temperatures are tabulated in Table I. The theoretical weight loss for reaction 2 is 22.8%, while that for the formation of $MoS_2$ from the combined reactions of eqs 2 and 5 is 29.8%. It appears from the data in Table I that the weight loss at ~300 °C

$$MoS_3 \xrightarrow[\Delta]{} MoS_2 + S \quad (4)$$

$$MoOS_2 \rightarrow MoS_2 + {}^1/_2O_2 \quad (5)$$

is close to that expected for the formation of $MoOS_2$. Our structural and electrochemical results discussed below, however, suggest that the compositions of the decomposition products of $(NH_4)_2MoO_2S_2$, isolated at different temperatures are more complex than those given by eqs 2 and 5.

In a series of experiments $(NH_4)_2MoO_2S_2$ was decomposed at 200, 300, 380 °C, and in a two-step thermolysis in which a first heating at 200 °C was followed by a second heating at 380 °C. Dark-gray solids, insoluble in organic solvents such as propylene carbonate and tetrahydrofuran, were obtained. All of the materials were amorphous solids, and consequently little information regarding their structures could be gathered from X-ray diffraction analysis. They behaved as reversible cathodes in secondary Li cells (vide infra) with their electrochemical behavior showing a dependence on the temperature at which they were formed. The cell potential versus capacity curves obtained for Li cells (vide infra) revealed that all of the oxysulfides, most probably, were single-phase materials. We have made an attempt to elucidate the compositions and structures of the oxysulfide from elemental analysis (Table II), and from both IR (Figures 2 and 3) and ESCA (Table III) spectral data. Elemental analysis was also obtained for the product of the decomposition of $(NH_4)_2MoS_4$ at 300 °C and it, as expected, was found to be $MoS_3$.

The decomposition of $(NH_4)_2MoO_2S_2$ at 200 °C yields a material with a composition of $MoOS_2$ but contains a significant amount of N and H which decreases as the decomposition temperature is raised. If the heating is carried out at 380 °C the stoichiometry of the product is closer to $MoO_{1.5}S_{1.5}$ than $MoOS_2$. It has been suggested previously[17] that over the temperature range 380–430 °C, $MoOS_2$ decomposes to form amorphous $MoS_2$ and oxygen. Our results seem to suggest that an oxysulfide is formed at temperatures as high as 380 °C. It appeared from a number of decomposition experiments that if the highest temperature is 300 °C or less for the first 3 h of the thermolysis, the product has a composition approaching $MoOS_2$. Infrared spectra of $(NH_4)_2MoO_2S_2$ and its decomposition products are presented in Figures 2 and 3, respectively. The sharp, clearly defined peaks at 835 and 800 $cm^{-1}$ in Figure 2 have been assigned to the Mo–O stretches of the $MoONH_4$ linkages, in accordance with structure 1. For the material prepared at 200 °C, a strong, sharp band at 939 $cm^{-1}$ is observed along with a broad band at ~780–800 $cm^{-1}$. As the thermolysis temperature is raised, the relative intensity of the sharp band decreases

(17) Prasad, T. P.; Diemann, E.; Müller, A. *J. Inorg. Nucl. Chem.* **1973**, *35*, 1895.

**Table II. Apparent Stoichiometry of Mo Oxysulfides Determined from Elemental Analysis**

| precursor | decomposition temp (°C) | apparent stoichiometry of product |
|---|---|---|
| $(NH_4)_2MoO_2S_2$ | 200 | $N_{0.4}H_{1.9}MoO_{1.0}S_{2.0}$ |
| $(NH_4)_2MoO_2S_2$ | 200–380 | $N_{0.2}MoO_{1.1}S_{1.8}$ |
| $(NH_4)_2MoO_2S_2$ | 300 | $N_{0.1}H_{0.7}MoO_{1.3}S_{1.7}$ |
| $(NH_4)_2MoO_2S_2$ | 380 | $N_{0.03}H_{0.3}MoO_{1.5}S_{1.6}$ |
| $(NH_4)_2MoS_4$ | 300 | $MoS_{3.0}$ |

**Table III. ESCA Results**

| sample | material description | S ($2p_{1/2}$) binding energy (eV) | Mo[b] ($3d_{5/2}$) binding energy (eV) |
|---|---|---|---|
| 1 | $(NH_4)_2MoO_2S_2$ | 162.1 | 230.2 |
| 2 | 200 °C dec of $(NH_4)_2MoO_2S_2$ | 162.4 | 230.3 |
| 3 | 200–380 °C dec of $(NH_4)_2MoO_2S_2$ | 162.5, 163.3 | 229.4 |
| 4 | 300 °C dec of $(NH_4)_2MoO_2S_2$ | 162.7 (broad)[a] | 230.3 |
| 5 | 380 °C dec of $(NH_4)_2MoO_2S_2$ | 162.6, 163.8 | 229.8 |

[a] The total width of this peak is the same as the combined widths of the peaks in sample 5. [b] All are doublets.

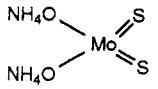

I

and it practically disappears at 380 °C. The broad peak at 780–800 $cm^{-1}$ remains in the materials prepared in a single step at temperatures ≤300 °C. In the material prepared in a single step at 380 °C this band is very weak and broad. Zhuang et al.[18] attributed broadening of this type observed in molecular oxomolybdenum compounds to the formation of oligomers in which the terminal oxygen of one monomer acts as a bridge to the Mo atom of another. The presence of nitrogen and hydrogen in some of the decomposition products together with their elemental composition and IR spectra can be explained by the reaction scheme represented by eqs 6–8. The product obtained at 200 °C, II, can be viewed as an oligomer of I with $-ONH_4$ end groups, whereas III is polymeric thiomolybdate.

$$\underset{\text{I}}{n(NH_4)_2MoO_2S_2} \xrightarrow{200\,^\circ C} \underset{\text{II}}{-(S_2MoO)_n-(O_{0.5}NH_4)_2} + (2n-2)NH_3 + (n-1)H_2O \quad (6)$$

$$\underset{\text{I}}{x(NH_4)_2MoO_2S_2} \xrightarrow{\sim 300\,^\circ C} \underset{\text{III}}{-(S_2MoO)_x-} + 2xNH_3 + xH_2O \quad (7)$$

$$\underset{\text{I}}{n(NH_4)_2MoO_2S_2} \xrightarrow{380\,^\circ C} \underset{\text{IV}}{-(S_{1.5}MoO_{1.5})_n-} + 2nNH_3 + 0.5nH_2O + 0.5nH_2S \quad (8)$$

The probable structures of II and III can be illustrated with the reaction schemes depicted in eqs 9 and 10. In III obtained at 300 °C, the $-ONH_4$ end groups mostly disappear and Mo–S bridging bonds appear. Material V obtained in a two-step process at 200/380 °C, differs from III only in the presence of $S_2$ bridges, whereas the material prepared in the one-step heating at 380 °C has both S and $S_2$ bridges along with equal amounts of O and S.

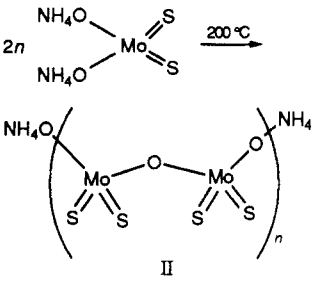

II

$$+ (2n-2)NH_3 + (n-1)H_2O \quad (9)$$

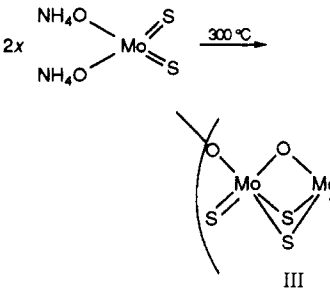

III

$$+ 2xNH_3 + xH_2O \quad (10)$$

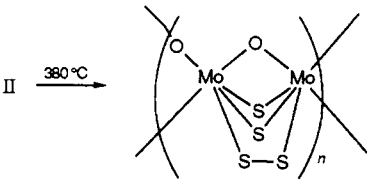

V

$$(11)$$

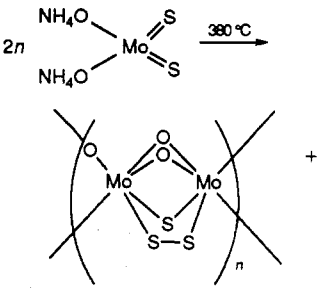

IV

$$+ 2NH_3 + 0.5nH_2O + 0.5nH_2S \quad (12)$$

Structures II–V are in reasonable agreement with the ESCA data for these materials presented in Table III. Sulfur can exist as either the monatomic ($S^{2-}$) or diatomic ($S^{2-}_2$) anion, and it is essential to establish the presence or absence of these in order to be able to assign structures with confidence. Jellinek et al.[19] have shown that the $2p_{1/2}$ sulfur levels give rise to different binding energies depending upon whether the S atoms are present as $S^{2-}$ or $S^{2-}_2$. For example, in $ZrS_3$, isolated $S^{2-}$ groups were found to have a binding energy of 162.7 eV, while the S–S pairs had a binding energy of 163.8 eV. For the spectra we have obtained, only the one for $(NH_4)_2MoO_2S_2$ approached the sharpness of one Jellineck reported for the $2p_{1/2}$ peak ($S^{2-}_2$) of $ZrS_2$. As a group, the spectra showed a definite trend; $(NH_4)_2MoO_2S_2$ and the oxysulfides formed at 200 and 300 °C had $S^{2-}$ ligands. The spectrum for the 300 °C product was as broad as that for the combined peaks for the 380 °C or the 200/380 °C product, suggesting both $S^{2-}$ and $S^{2-}_2$ are present when temperature ≥300 °C are used to form oxysulfides from $(NH_4)_2MoO_2S_2$. The Mo binding energies suggested first that all the materials are all single phases. The highest value is for $(NH_4)_2MoO_2S_2$, in agreement with the fact it contais $Mo^{(VI)}$. The 200 and 300 °C materials

(18) Zhuang, B.; McDonald, J. W.; Newton, W. E. *Inorg. Chim. Acta* **1983**, *77*, L221.

(19) Jellinek, F.; Pallak, R. A.; Shafer, M. W. *Mater. Res. Bull.* **1987**, *22*, 37.

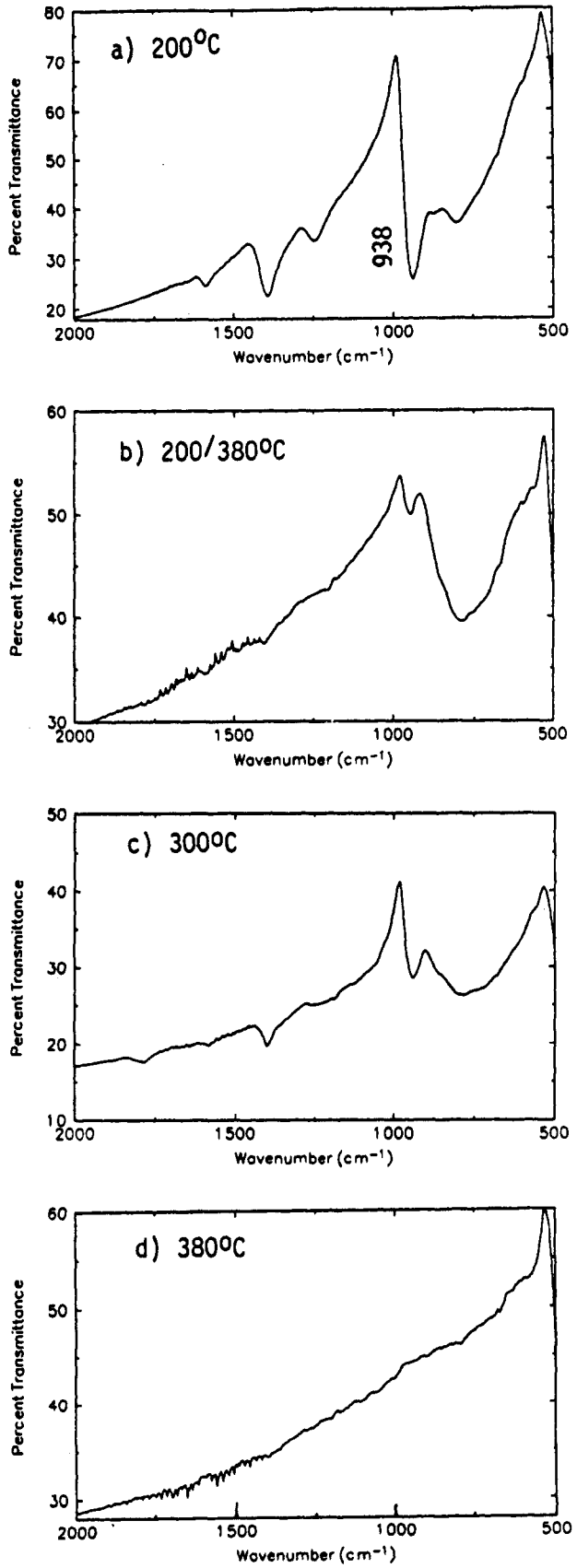


**Figure 3.** FTIR spectrum of molybdenum oxysulfides obtained from the decomposition of $(NH_4)_2MoO_2S_2$ at different temperatures.

had Mo binding energies very close to that for $(NH_4)_2MoO_2S_2$, which are consistent with the structures II and III. For the materials obtained from the 380 °C heating, the binding energies have lower values and are suggestive of some $Mo^V$ character. It is useful to compare here the proposed structures of Mo oxysulfides with that of $MoS_3$. It has been proposed from EXAFS data[20] that $MoS_3$ is formulated properly as $Mo_2^V(S^{2-}{}_2)(S^{2-})_4$ with both monoatomic and diatomic sulfides and Mo–Mo bonding. The proposed structures of the oxysulfides formed at temperatures ≥300 °C contain both $S^{2-}$ and $(S^{2-}{}_2)$; but whether or not they have Mo–Mo bonding remains to be established.

**Table IV. Results for Chemical Lithiation of $MoS_2$, $MoS_3$, and $MoO_xS_y$**

| material | Li/Mo | material | Li/Mo |
|---|---|---|---|
| $MoS_2$ | 1.1 | $MoO_xS_y$(300) | 3.4 |
| $MoS_3$ | 4.0 | $MoO_xS_y$(200–380) | 3.5 |
| $MoO_xS_y$(200) | 3.1 | $MoO_xS_y$(380) | 2.5 |

We have found that an oxysulfide of the compositions $MoO_{0.8}S_{2.1}$ (with small amounts of N and H) could be prepared from the solid-state decomposition of a 1:1 mole mixture of $(NH_4)MoS_4$ and ammonium paramolybdate. First of all, the two ammonium molybdates were mixed in aqueous $NH_3$ and stirred well to form a homogeneous solution, and the $NH_3$ was then removed by evaporation to obtain the solid precursor. The solid residue was then decomposed at 300 °C, and the oxysulfide formed had an IR spectrum similar to that for the material prepared at the same temperature from $(NH_4)_2MoO_2S_2$. In addition, it exhibited an ESCA spectrum with $Mo3d_{5/2}$ at 230.2 eV and S $2p_{1/2}$ at 162.8 eV. These data together with its electrochemical behavior suggest that a Mo oxysulfide was indeed formed. A condensation–polymerization reaction involving the molybdate and thiomolybdate in the solid-state at 300 °C explains the formation of the oxysulfide. It should be noted that UV–visible spectra of solutions of mixtures of $(NH_4)_2MoS_4$ and ammonium paramolybdate in aqueous $NH_3$ indicated no evidence for the formation of $(NH_4)_2MoO_2S_2$ after stirring for 1 week at room temperature, followed by refluxing for 4 h. On the other hand, the formation of a molybdenum oxysulfide by the solid-state route from the molybdate mixture suggests the possibility of preparing novel materials of controlled stoichiometry from judiciously selected precursor mixtures.

**Electrochemistry of Molybdenum Oxysulfides in Lithium Cells.** The usefulness of the molybdenum oxysulfides as cathodes for rechargeable Li cells was assessed from their reactions with *n*-BuLi and discharge/charge behavior in Li cells.

The reducing power of *n*-BuLi, expressed in the electrochemical scale, is approximately 1 V versus $Li^+/Li$.[21] Thus the amount of *n*-BuLi reacted with a given oxysulfide provides information about the cathode material's capacity corresponding to its discharge to a potential of 1 V in a Li cell. The reaction with *n*-BuLi may involve an insertion or a displacement process, a distinction between the two can be made only from an analysis of the reaction products. In the former case, a solid solution is formed as the product,[1] whereas for the latter, the products could be $Li_2O$, $Li_2S$, or both along with the reduced Mo specie. Pertinent data are presented in Table IV. The reactions of $MoS_2$ and $MoS_3$ with *n*-BuLi were carried out for comparison and the results are in good agreement with

(20) Scott, R. A.; Jacobson, A. J.; Chiannelli, R. R.; Pan, W. H.; Stiefel, E. I.; Hodgson, K. O.; Cramer, S. P. *Inorg. Chem.* **1986**, *25*, 1461.
(21) Murphy, D. W.; Christian, P. A. *Science* **1979**, *205*, 651.

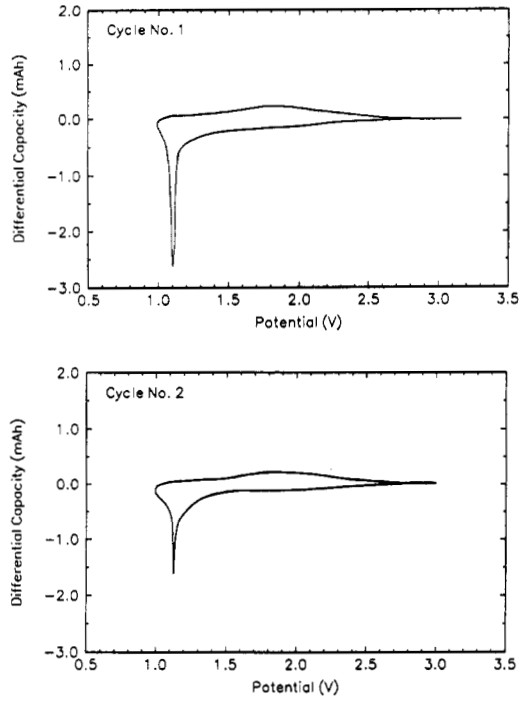


**Figure 4.** First two cycles by the potential-step cycling of Li/$MoO_xS_y$(380) cell. The electrolyte was PC/$LiClO_4$.

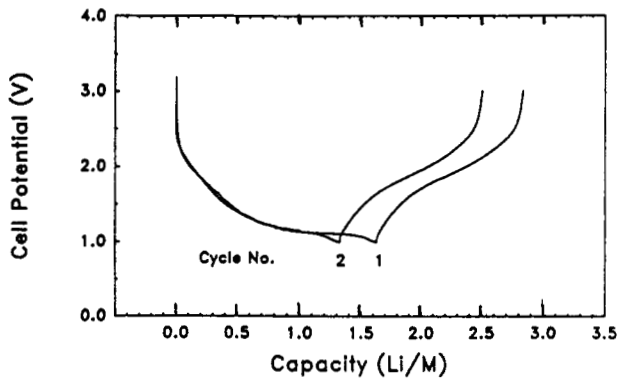


**Figure 5.** First two cycles in Figure 4 plotted as cell potential versus capacity.

published data.[6,10] X-ray analysis of the products did not show the presence of either $Li_2S$ or $Li_2O$. We conclude from the absence of these materials in the X-ray data that molybdenum oxysulfide reactions with Li (eqs 13 and 14) involve an insertion process.

$$z\text{BuLi} + MoO_xS_y \rightarrow Li_xMoO_xS_y + {}^1/_2zC_8H_{18} \quad (13)$$

$$zLi + MoO_xS_y \rightarrow Li_xMoO_xS_y \quad (14)$$

The electrochemical data described below also strongly suggest insertion of Li into $MoO_xS_y$.

**Li/$MoO_xS_y$ Cells.** The stepped-potential cycling data for a cell utilizing the material prepared at 380 °C from $(NH_4)_2MoO_2S_2$, hereafter referred to as $MoO_xS_y$(380), are presented in Figures 4 and 5. The voltage limits were 1.0 and 3.0 V; i.e., the cell was first discharged in each cycle to a voltage limit of 1.0 V, and then charged to 3.0 V. The cell capacity is expressed as moles of lithium inserted per mole of molybdenum in the oxysulfide, i.e., Li/Mo. The capacity in the first discharge was 1.63 Li/Mo, and of this about 1 Li appeared in the sloping region between 2.0 and 1.0 V and the rest at a plateau of about 1.15 V. About 1.20

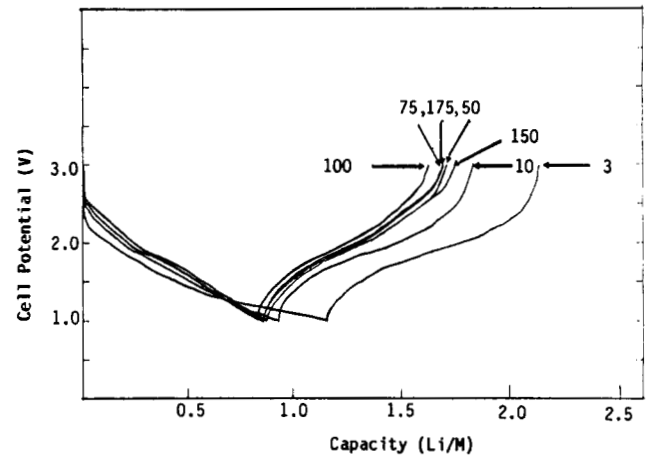


**Figure 6.** Galvanostatic charge/discharge cycles of Li/$MoO_xS_y$(380) cell. Current density was ±0.25 mA/cm²; electrolyte was PC/$LiClO_4$.

Li/Mo, i.e., ~75% of the capacity in the first discharge, was rechargeable. The gradually downward sloping potential profile appearing with the degree of Li insertion is indicative of a single-phase reaction at least down to a potential of about 1.2 V. That is to say, before and after Li insertion $MoO_xS_y$ has the same short-range crystallographic structure. For the first cycle, the charge curve has a more sloping profile than the discharge curve, and the cause of this is not understood well at this time. In view of the fact that on a carbon electrode, PC undergoes reduction at about 1.0 V versus Li/Li,[22] it is tempting to ascribe the irreversible capacity in the first discharge to the reduction of this solvent. Indeed a reduction peak is observed in Figure 4 at about 1.15 V, and the current involved in it decreases from the first to the second discharge. Nevertheless, we cannot rule out that a fraction of the irreversible capacity in the first discharge is due to the difficulty in extracting the Li that is initially inserted into $MoO_xS_y$. An examination of the ratio of the charge to discharge capacity as a function of cell potential suggests that some of the capacity observed at the 1.15-V discharge plateau is indeed due to Li insertion into $MoO_xS_y$. The discharge/charge ratio became closer in the second cycle and remained nearly 100% for many cycles thereafter.

The long-term cycling data, determined from galvanostatic discharge/charge cycling, presented in Figure 6, support the rechargeability of $MoO_xS_y$(380). More than 175, full depth, discharge/charge cycles were obtained with only a small decrease in capacity from the 10th cycle onward. The cell, however, lost about 20% of its capacity between the second and the ninth cycle. This we believe is due to a combination of factors: Capacity losses in secondary Li cells occur from irreversible Li insertion processes, parasitic reactions (for example, involving electrolyte), and associated impedance increases in the cell as well as changes in the physical structure of the porous cathode and related kinetic limitations. Repeated Li insertion/extraction processes can cause some of the cathode particles to become isolated from the bulk of the material in the electrode and lose electronic contact. The cell capacity will decrease in proportion to the amount of the cathode that becomes electrochemically isolated from the bulk. Usually this occurs in the first several cycles as it is then that the cathode particles make major positional

(22) Dey, A. N.; Sullivan, B. P. *J. Electrochem. Soc.* **1970**, *117*, 222.

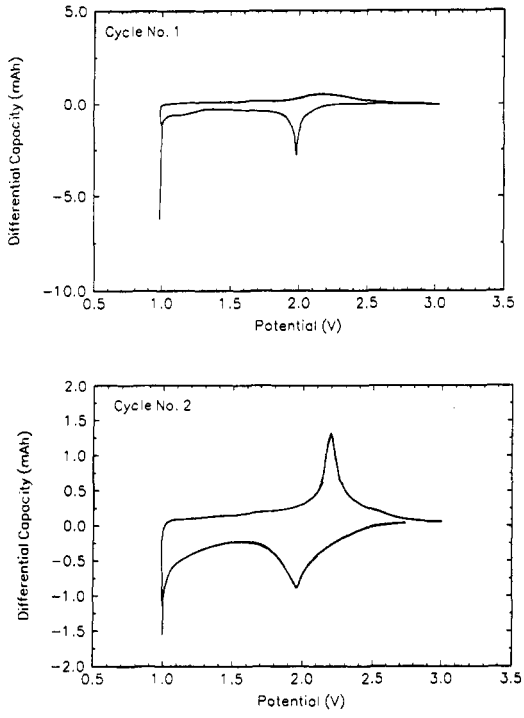


**Figure 7.** First two cycles obtained by the potential-step cycling of Li/$MoO_xS_y$(200/380) cell. Electrolyte was PC/$LiClO_4$.

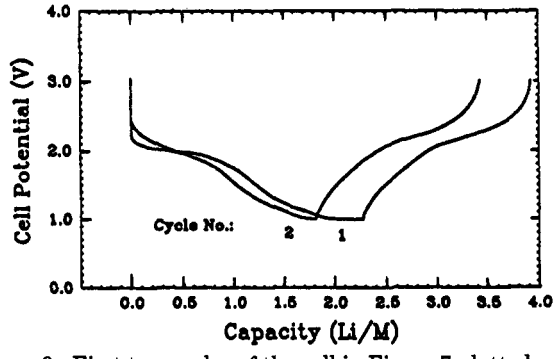


**Figure 8.** First two cycles of the cell in Figure 7 plotted as cell potential versus capacity.

adjustments; subsequently they acquire their equilibrium positions whereby little change in electrode structure-related capacity loss may occur.

Figures 7 and 8 display the cycling data of the Mo–oxysulfide obtained from the 200/380 °C thermolysis of $(NH_4)_2MoO_2S_2$. In this case the capacity observed at 1.0 V most probably is due to electrolyte solution reduction as practically all of this capacity is irreversible. When this capacity of 0.38 Li/Mo at the 1.0 V plateau is subtracted from the total capacity in the first discharge the cathode yields a capacity of 1.90 Li/Mo, which is reversible. For the second cycle the discharge yielded 1.82 Li/Mo while the recharge was 1.6 Li/Mo. Figure 9 depicts the long-term cycling of another cell utilizing this material. Again, the cycling data indicate the rechargeability of this positive electrode. Since the cell contained the ether-based electrolyte, discharge was performed to a cutoff voltage limit of 1.6 V, which explains the smaller capacity of this cell as compared to the capacity of the cell in Figure 8.

The electrochemical performances of the materials obtained from the 300 and 200 °C decompositions, respectively, of $(NH_4)_2MoO_2S_2$ are illustrated in Figures 10–13. These materials exhibited higher capacities initially

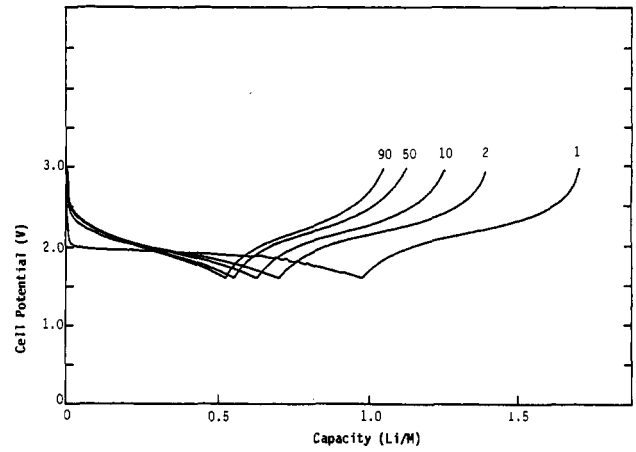


**Figure 9.** Galvanostatic charge/discharge cycling curves for a Li/$MoO_xS_y$(200/380) cell. Current density was ±0.25 mA/cm$^2$; electrolyte was the ether solution.

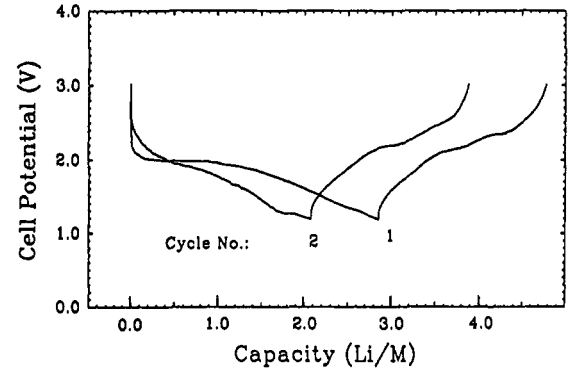


**Figure 10.** First two cycles obtained by potential-step cycling of Li/$MoO_xS_y$(300) cell. Electrolyte was PC/$LiClO_4$.

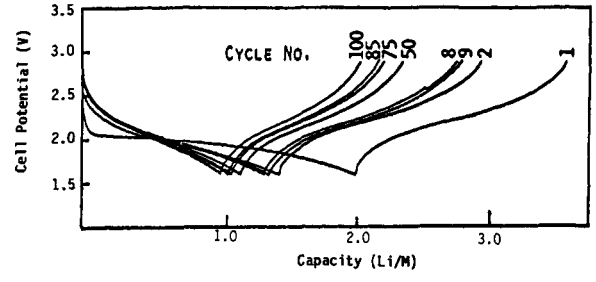


**Figure 11.** Galvanostatic cycling curves for a Li/$MoO_xS_y$(300) cell containing THF:2Me–THF:2Me–F/$LiAsF_6$ electrolyte. Current density was 1.0 mA/cm$^2$ for cycles 1, 2, and 8 and ±0.5 mA/cm$^2$ for all others.

than those obtained from the materials prepared at higher temperatures; the increased capacities appearing at about the 2-V plateau. While these cathodes performed well during long-term cycling, as demonstrated by the data in Figures 11 and 13, the capacity loss in the initial cycles was higher than those of the higher temperature oxysulfides. Another noticeable behavior is the change in the discharge potential profile upon going from the first to the second cycle. The plateau at ~2 V practically disappears in the second discharge and the potentials become more sloping with increasing Li insertion. This behavior can be ascribed to a phase change in the material. A careful examination of the cycling curves reveals that the phase change probably takes place in the first discharge since a sloping potential profile appears beginning with the first charge, and the second discharge shows a mirror image profile of the first charge. Such phase changes

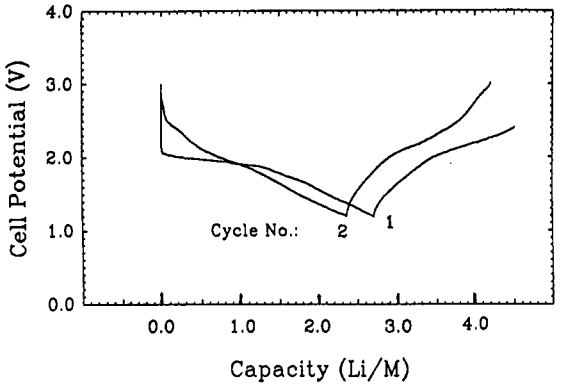


**Figure 12.** First two cycles obtained by potential-step cycling of $Li/MoO_xS_y(200)$ cell. The electrolyte was $PC/LiClO_4$.

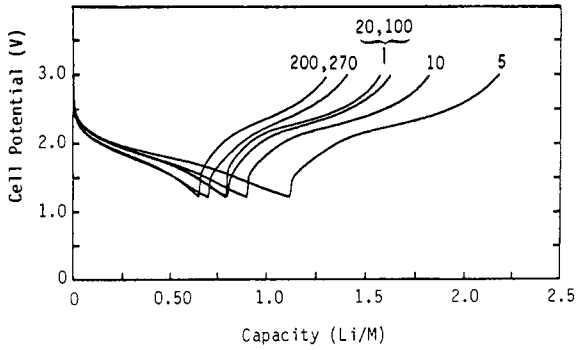


**Figure 13.** Galvanostatic cycling curves of the cell in Figure 12. Current density was ±0.25 mA/cm². The electrolyte was $PC/LiClO_4$.

concurrent with Li insertion have been established in $MoS_2$ where the material changes from a 2H–$NbS_2$ to a 1T–$CdI_2$ structure upon Li insertion.[23] The latter structure apparently is maintained during subsequent cycling provided a small amount of Li is retained in $MoS_2$ at the completion of each charge half-cycle. A similar behavior has also been exhibited by 2H–$NbS_2$ during Na insertion in a $Na/NbS_2$ battery.[24] The unusual aspect of the phase transformation accompanying Li insertion in the molybdenum oxysulfides is that the hosts are amorphous compounds, whereas $MoS_2$ and $NbS_2$ are crystalline materials. The phase structures involved in the molybdenum oxysulfides are not well understood at this time, and their elucidation will require the use of more sophisticated analytical techniques than those we have employed. Since amorphous materials lack long-range crystalline order and the associated electronic band structures, the phase transformations may be viewed in the same manner as that of a molecular structure. In this case, however, the relationship observed between molecular structure and cathode potential is intriguing and invites further investigation. The $MoO_xS_y(380)$ appears to be quite distinct from the other materials in that its potential shows a monotonic decrease with the degree of Li insertion and there is apparently little or no phase change from the first to the second discharge. It will be recalled that the 380 °C decomposition product of $(NH_4)_2MoO_2S_2$ has been described previously as $MoS_2$.[17] Both our analytical results and cycling data indicate otherwise. The discharge and charge curve obtained with

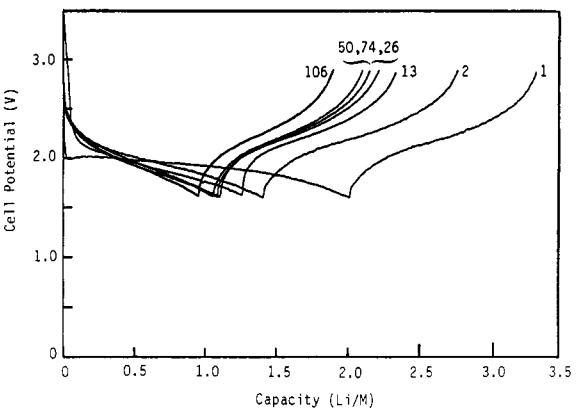


**Figure 14.** Galvanostatic cycling curves for a $Li/MoO_xS_y$ cell in which the oxysulfide was obtained from the decomposition of a mixture of $(NH_4)_2MoS_4$ and $(NH_4)_2MoO_4$. Current density was ±0.5 mA/cm². The electrolyte was the ether solution.

amorphous $MoS_2$[25] is very different from the one we obtained with $MoO_xS_y(380)$. The same data for the 380 °C material, however, seem to indicate that the phase it acquired after the first discharge is different from the phase(s) of the lower temperature materials at similar conditions. It may be then argued that the electrochemical reactions of the lower temperature materials convert them to a more stable phase, perhaps by removal of some of the oxygen or sulfur or both as $Li_2S$ and $Li_2O$. These Li compounds, formed as minor products in the first discharge could remain amorphous and therefore escaped detection by X-rays. On the other hand, the formation of a stable $Li_xMoO_xS_y$ phase without its decomposition to $Li_2S$ or $Li_2O$ is also plausible.

Figure 14 depicts the discharge/charge cycles for the material prepared from a mixture of $(NH_4)_2MoO_4$ and $(NH_4)_2MoS_4$, by thermolysis at 300 °C. The discharge potential profile versus the degree of Li insertion is very much similar to that of $MoO_xS_y(300)$. A single-phase material is indicated by the first discharge curve free of potential steps, and the change in the profiles of the first discharge to the first charge curve suggests that as with $MoO_xS_y(300)$ apparently there is a phase change accompanying the first discharge. A capacity-loss of about 25% occurs from the second discharge onward, but the material has excellent rechargeability. It appears that molybdenum oxysulfides can be prepared by the direct solid state decomposition of mixtures of $(NH_4)_2MoO_4$ and $(NH_4)_2MoS_4$, and this procedure then provides a more direct route to the synthesis of oxysulfides in which the ratio of O to S may be varied by adjusting the ratio of the two ammonium compounds taken initially.

## Conclusions

Molybdenum oxysulfides have been identified as a new class of amorphous host materials capable of topochemically reacting with Li. The extent of Li insertion and the chemical reversibility of the process appeared to depend on the temperature at which they were formed from $(NH_4)_2MoO_2S_2$. Thermolysis of the latter apparently results in a solid-state polymerization reaction leading to a variety of molybdenum oxysulfides whose compositions and Li insertion chemistry were very much sensitive to

(23) Py, M. A.; Haering, Q. R. *Can. J. Phys.* **1983**, *61*, 76.
(24) Abraham, K. M.; Pitts, L.; Schiff, R. *J. Electrochem. Soc.* **1980**, *127*, 2545.
(25) Auborn, J. J.; Barberio, V. L.; Hanson, K. J. *J. Electrochem. Soc.* **1987**, *134*, 580.

**Table V. Specific Energies of Secondary Li Battery Couples As Determined from First Discharge**

| cathode | capacity (Li/Mo) | middischarge voltage (V) | quasi-theoretical[a] specific energy[b] (W h/kg) |
|---|---|---|---|
| $MoS_2$ | 1.0 | 1.7 | 272 |
| $MoS_3$ | 3.0 | 1.9 | 720 |
| $MoO_xS_y(200)$ | 2.7 | 1.8 | 629 |
| $MoO_xS_y(300)$ | 2.9 | 1.9 | 685 |
| $MoO_xS_y(200/380)$ | 2.0 | 1.9 | 670 |
| $MoO_xS_y(380)$ | 1.1 | 1.2 | 290 |

[a] Specific energy = cell voltage (V) × cell capacity (A h)/weight of cell (kg). [b] Based on cell capacity and voltage and weights of the reactants only. The weights of the hardware and electrolyte are not included. Usually about 20–30% of this energy can be obtained in practical cells.

the temperature at which they were formed. The resulting molybdenum oxysulfides can be viewed as polymers of $(NH_4)_2MoO_2S_2$ with different chain lengths or molecular weights. The phase transformations accompanying Li insertion in some of the oxysulfides have precedence in layered crystalline transition-metal chalcogenides and is intriguing considering the amorphous structures of the materials.

The potential utility of the molybdenum oxysulfides as reversible cathodes for rechargeable Li batteries is exemplified by the specific energy data presented in Table V. Three of the oxysulfides compare favorably with $MoS_3$. The substantial development work previously carried out in this laboratory on $MoS_3$ indicated[5] a high rate of capacity loss with cycling for this electrode. The capacity retention with cycling of the molybdenum oxysulfides, however, is much better, and this together with energy densities suggest that further studies of the structure and properties of these new class of materials should be pursued. For example, novel materials with interesting chemical and electrochemical properties could be prepared by the condensation of $(NH_4)_2MoO_3S$ alone or together with $(NH_4)_2MoO_2S_2$. Further, materials with intriguing solid-state chemistry and electrochemistry may be formed with the use of transition metals other than Mo.

**Acknowledgment.** This work was carried out with financial support from U.S. Army Laboratory Command, Fort Monmouth, NJ, under Contract DAAL01-88-C-0844.